Dynamics of an Ultrasonic Transducer Used for Wire Bonding

S. W. Or, *Member, IEEE*, H. L. W. Chan, V. C. Lo, *Member, IEEE*, and C. W. Yuen

***Abstract*—The vibration displacement distributions along a transducer used in ultrasonic wire bonding were measured using a heterodyne interferometer, and many nodes and anti-nodes were found. A mechanical finite element method (FEM) was used to compute the resonant frequencies and vibration mode shapes. The displacement distributions of the dominant 2nd axial mode agreed well with the measured values. Undesirable nonaxial modes, including the higher order flexural and torsional modes, also were excited at frequencies very close to the working frequency (2nd axial mode) of the transducer. Hence, the measured displacements were the resultant of all the allowable modes being excited. However, the excitation of these nonaxial modes were small enough not to affect the formation of consistent and high quality wire bonds. Results of the present study were used to determine a suitable location for installing a piezoelectric sensor to monitor the bond quality.**

I. Introduction

Wire bonding is a widely used method of chip interconnection in the microelectronics industry. Historically, it has been used in all chip packaging styles ranging from small individual chip packages in the late 1950s to today's large, high-density multi-chip modules [1]. Variation in bonding quality has been a concern; but conventional bond quality assurance techniques, such as the pull test and the shear test, are destructive, expensive, and time consuming [2]. As the degree of automation in bonding process and the range of bonding parameters increase, there is a need to develop a real-time automatic process control system. Installing a piezoelectric sensor on the transducer is a possible way to provide a real-time signal for feedback control. In order to find a suitable location for sensor placement, it is necessary to understand the vibration characteristics of the particular transducer system first.

Simplified models describing the mechanical behavior of an ultrasonic transducer used in wire bonding have been reported in many previous work [3]–[8]. They are useful for predicting general characteristics, but are not capable of describing detailed behavior of individual transducer design. Using state-of-the-art interferometry measurement and FEM modeling, information pertinent to a particular transducer system can be obtained and used as a guide to install sensor for automatic process control.

Some preliminary work by us on using a piezoelectric sensor attached to a transducer to monitor bond quality has been reported [9]. More detailed modeling is presented here, as well as how we find a suitable location for the piezoelectric sensor placement.

Manuscript received March 25, 1997; accepted February 2, 1998. Financial support from The Hong Kong Polytechnic University Teaching Company Scheme (TCS) is acknowledged.

S. W. Or, H. L. W. Chan, and V. C. Lo are with the Department of Applied Physics and Materials Research Center, The Hong Kong Polytechnic University, Hunghom, Kowloon, Hong Kong (e-mail: swor@asmpt.com).

C. W. Yuen is with ASM Assembly Automation Ltd., Kwai Chung, Hong Kong. S. W. Or also is with ASM.

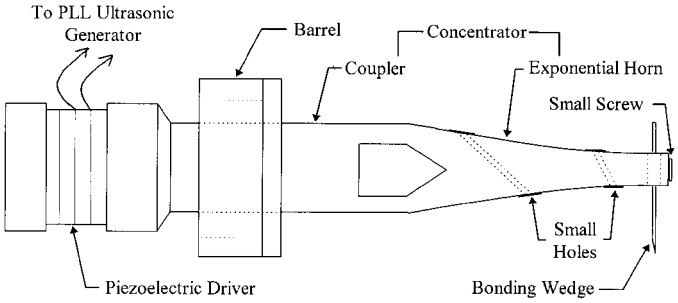

Fig. 1. Diagram of ultrasonic transducer used for wire bonding.

II. Ultrasonic Transducer Used For Wire Bonding

An ultrasonic transducer converts electrical energy into mechanical vibration. As shown in Fig. 1, the concentrator (coupler and exponential horn) and bonding wedge (which is clamped into a hole drilled at the front end of the horn by a small screw) are driven by the output of a phase-locked-loop (PLL) ultrasonic generator. The axial vibration obtained from the piezoelectric driver is transmitted and amplified by the concentrator. The wave is converted to flexural vibrations in the bonding wedge and is transmitted to the bond interface during the bonding process. The length of the concentrator is usually adjusted to one wavelength at the resonant frequency of the piezoelectric driver, which was about 60 kHz in the present study. The profile of the exponential horn also is tailored to provide the desired gain factor to amplify the motion. A barrel, which is used for mounting the transducer on the bonder, is positioned at the node of the coupler to avoid energy loss. There are two small holes in the concentrator for threading the Al wires which are drilled at 60° and 30°, respectively.

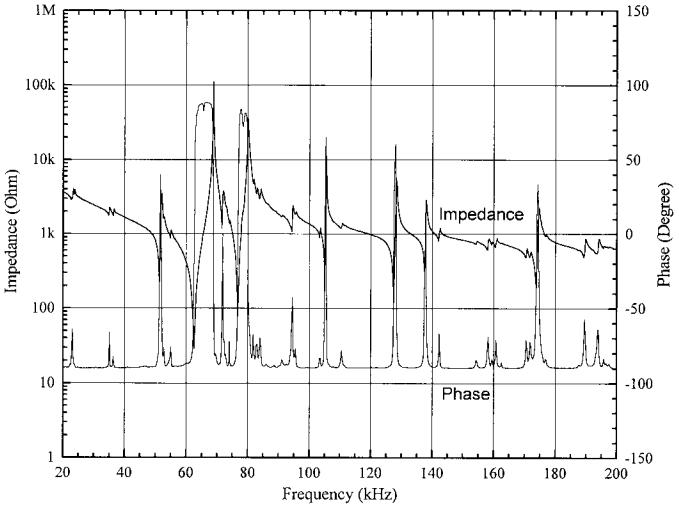

Fig. 2. Electrical impedance and phase angle as functions of frequency for the ultrasonic transducer.

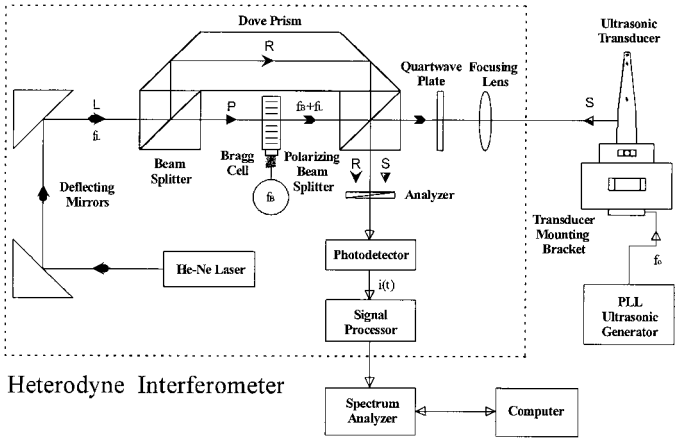

Fig. 3. Experimental setup for vibration displacement distribution measurements.

III. Resonance Characteristics of the Ultrasonic Transducer

The electrical impedance and phase angle as functions of frequency (Fig. 2) were measured using an HP 4149A Impedance/Gain Phase Analyzer with the ultrasonic transducer being clamped in the wire bonder. The results show that the transducer has a number of allowable resonant frequencies (or vibration modes). The strongest minimum impedance resonance is observed at 62.5 kHz which is the operating frequency of the transducer (nominal value is 62.1 to 62.8 kHz) and the PLL ultrasonic generator should be tuned to lock at this point in order to maintain resonance. Coupling between adjacent modes and a number of weaker resonances, including the higher frequency harmonics of the fundamental and those with frequencies very close to it (within $\pm$ 2 kHz of the transducer operating frequency) also can be observed. If these different (spurious) modes are excited as well, they may influence the transducer vibration and affect the bond quality.

IV. Vibration Displacement Distribution Measurements Using a Laser Interferometer

A. Principle of Detection

A Mach-Zehnder type heterodyne interferometer (SH-120 from B. M. Industries in France) [10] was used to measure the ultrasonic displacements along the concentrator surface (Fig. 3). A horizontally polarized laser beam (frequency f_L; wave number $k = 2\pi/\lambda$, wavelength $\lambda =$ 6328 Å for a He-Ne laser) is split into a reference beam R and a probe beam P. The reference beam is directed through a dove prism into a photodiode. The frequency of the probe beam is first shifted by f_B (70 MHz) in a Bragg cell, and the reflected beam S is then phase modulated by the ultrasonic displacement of the transducer $\phi(t)$. For a sinusoidal displacement of the surface $\phi(t) = u[\sin(\omega_o t)]$, where u and ω_o are the ultrasonic displacement and angular frequency ($\omega_o = 2\pi f_o$) of the transducer, respectively, the interference of two beams on the photodetector delivers a beat signal proportional to $\cos[\omega_B t + (2ku)\sin(\omega_o t)]$. The frequency spectrum of this signal contains sidebands at frequencies $\omega_B \pm n\omega_o$, where $n = 1, 2, 3, \ldots$. Each sideband has a relative amplitude equal to the Bessel function $J_n(x)$, where $x = 4\pi u/\lambda$. The ratio R_n between the carrier level $J_0(x)$ and the sideband levels $J_n(x)$ provides an absolute amplitude of the ultrasonic displacement. That is,

$$R_n = 10^{R_n'/20} = J_n(x)/J_0(x) \quad n = 1, 2, 3 \ldots$$

The value of R_n' in dBm can be read from a spectrum analyzer (HP 3589A). Then, R_n in linear scale is obtained and hence the unknown x. The ultrasonic displacement is:

$$u = x\lambda/4\pi.$$

The photon noise limits the detectivity to 10^{-4} Å, for a 1 Hz detection bandwidth [10]. For a 35 MHz bandwidth, the minimum detectable displacement is about 0.6 Å. From Bessel function of the 1st kind, at $x \approx 2.4$, $J_0(x)$ will be zero [11]. Thus, x is limited to this value in practice. For small displacements (i.e., $u < 100$ Å), only the components at f_B and $f_B \pm f_o$ are significant [12].

B. Displacement Distributions Along the Concentrator

Experimentally, the transducer was clamped on a micromanipulator capable of moving in the x, y, z, and θ directions. The orientation of the transducer was adjusted so that the laser beam was normal to the vibration surface and maximum signal level on the spectrum analyzer was obtained. The driving voltage was 3.7 $V_{p\text{-}p}$ for optimum bonding condition. The vibration displacement distributions along the concentrator (coupler and exponential horn) at 62.5 kHz (the transducer operating frequency) were measured, in steps of 0.5 mm, along the dotted lines

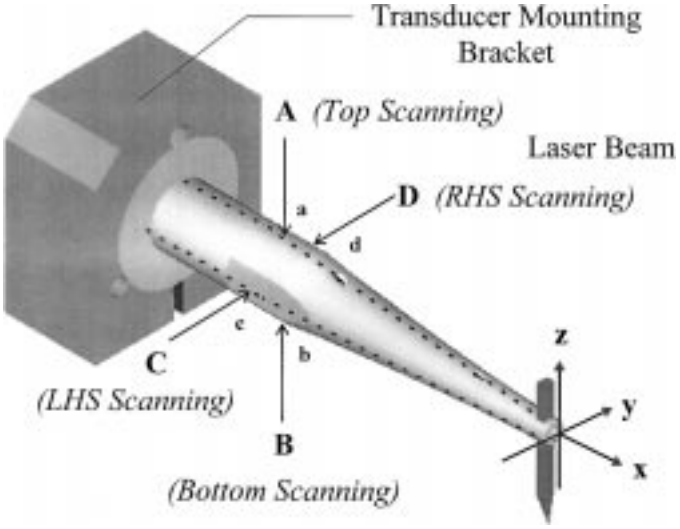

Fig. 4. A 3-D diagram of the ultrasonic transducer.

'a' (top scanning), 'b' (bottom scanning), 'c' (LHS scanning), and 'd' (RHS scanning), while the laser beam impinged on the transducer along directions 'A', 'B', 'C', and 'D', respectively (Fig. 4).

The rod waves excited in the transducer give rise to many nodes and antinodes along the surface of the concentrator. The measured amplitudes in Fig. 5 show that the displacement nodes and antinodes in the LHS and RHS scannings are located at similar locations on the concentrator. However, the displacement nodes and antinodes for the top and bottom scannings are 180° out of phase in the first 20 mm (coupler), and at more or less the same locations in the last 40 mm section (exponential horn). The mismatch in the first 20 mm may be due to the asymmetric 3-line clamping and the lack of geometric symmetry of the transducer. The degree of similarity increases toward the bonding wedge in order to satisfy the common boundary conditions at the end of the horn. Displacement patterns for the top and bottom scannings are different from those for side scannings and amplification of displacement by the exponential horn is also observed.

The error of this experiment by comparing the results of $J_1(x)/J_0(x)$ to those of $J_2(x)/J_0(x)$ (not shown) is about 10%. This indicates that the excitation of spurious modes in the transducer is still low compared to the excitation of the fundamental resonance. The measurements are typically reproducible to within about 20%.

In order to control the vibration characteristics of the transducer, it is usually designed specifically to facilitate bonding by an axial motion. In practice, however, due to loading of the massive piezoelectric driver and variation in clamping conditions, various spurious modes can still be excited in the transducer. Because the interferometer measures the absolute vibration amplitude normal to the transducer surface, the vibration displacement distributions measured are the resultant of all the allowable modes being excited, with the fundamental axial mode being dominant.

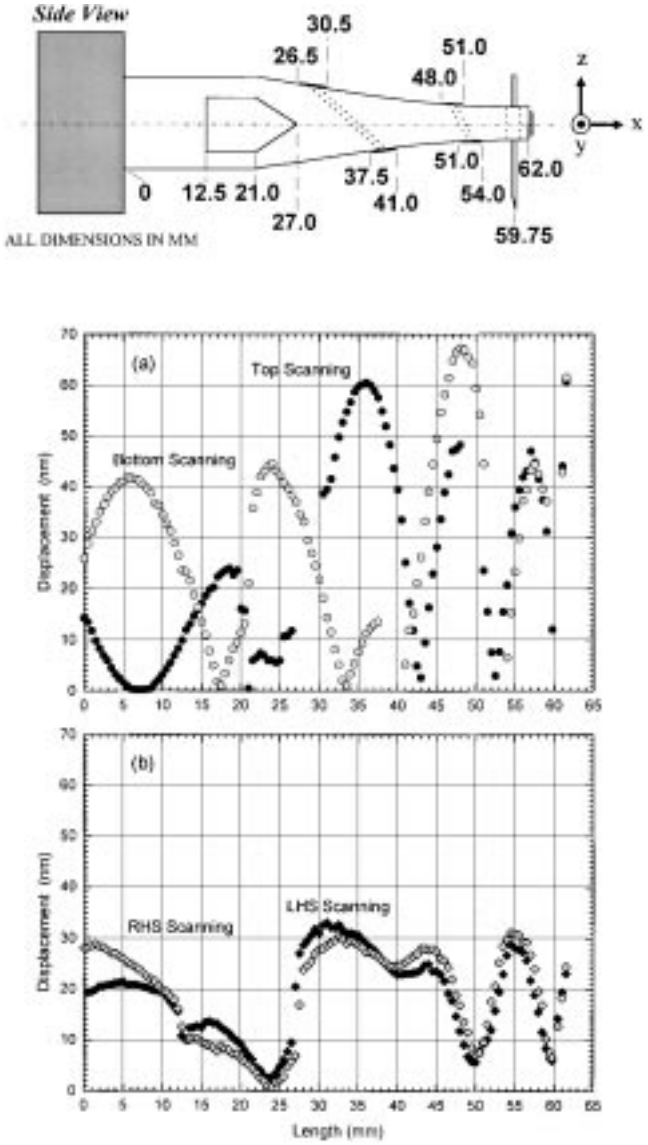

Fig. 5. Vibration displacement distributions along the concentrator of the transducer. (a) Top (solid circle) and bottom (open circle) scannings; (b) LHS (solid diamond) and RHS (open diamond) scannings.

V. Modal Analysis Using Finite Element Method

A. FEM Model

The resonant frequencies and vibration mode shapes of the ultrasonic transducer were computed using ANSYS 5.2. With the piezoelectric effect being neglected, a mechanical FE model is used (Fig. 6). The concentrator is made of Al alloy, and the driver is simplified to be a cylinder with the same stiffness as that of the concentrator. The tungsten carbide wedge also was simplified to be a cylindrical beam. Densities of the driver and the wedge are selected in a way that, when combined with the volume, will give the actual mass of these two components.

Moreover, small holes and fillets in the concentrator and screw for mounting the wedge to the concentrator are ig-

Fig. 6. Finite element model of the ultrasonic transducer.
Fig. 7. Mode shapes of the possibly excited modes. Note that only the dominant component (x, y, or z) of that mode is plotted. Amplitude of each mode is only the relative value in that particular mode. There is no absolute calibration, so each mode cannot be directly compared. (a) Second axial mode (mode 59—62.2 kHz), (b) flexural (lateral) mode (mode 60—63.3 kHz), (c) flexural (vertical) mode (mode 61—63.8 kHz), and (d) complex flexural (lateral) torsional mode (mode 62—64.4 kHz).

nored because of difficulty in meshing. All parts in the assembly are assumed to have perfect mechanical coupling to the horn. Fixed boundaries are assumed on the cylindrical surface of the barrel instead of the 3-line clamping.

The 17911 3-D structural solid elements solid 92 (10-node tetrahedral) and 29501 nodes are used for the analysis, and the h-method [13] is applied to model the highly curved volume. Meshing is restricted by the length of element which is set to 0.8 mm to 1.4 mm, depending on the volume of interest and the shape of the element. The maximum degree of freedom is 83679. The CPU time is 17260 seconds on a computer using Intel Pentium Pro 200 MHz CPU, 128 MBytes RAM.

B. FEM Results and Discussion

The natural frequencies of the first 120 modes are computed and compared to the impedance spectrum in Fig. 2. Some of the computed modes were found to be excluded by the electrical boundary conditions and are not observed in the spectrum. The computed mode shapes can be categorized as follows or as a combination of them (complex mode due to the effect of mode coupling): axial, which causes the tip of the wedge to move in a direction parallel to the axis of the concentrator (x-axis); flexural (lateral motion), which causes the tip of the wedge to move from side to side (y-axis); flexural (vertical motion), which causes the tip of the wedge to move up and down (z-axis); and torsional, which causes the concentrator to twist and the wedge to expand at the tip.

The computed modes with frequencies within 5% of the measured operating frequency of the transducer (62.5 kHz) are listed in Table I, and the corresponding mode shapes are shown in Fig. 7. The computed working frequency is 62.2 kHz (mode 59—2nd axial mode), which is in good agreement with the measured value (agreed to 0.48%). The first axial mode is found at 27.0 kHz (mode 34). Moreover, two higher order flexural modes and a complex mode are found at frequencies very close to the transducer operating frequency.

In practice, all these modes are excited simultaneously, and the undesirable modes are difficult to eliminate completely. The axial vibration is the most desirable motion in the ultrasonic Al wedge bonding and should be the working vibrational mode of the transducer. Lateral flexural motion from side to side and torsional motion would deteriorate the bond quality, but they still can keep the bonding wedge in contact with the wire. Vertical up and down flexural motion is the most undesirable because it tends to separate the bonding wedge from the wire. Therefore, it is important to find out whether the amplitudes of these undesirable modes are low enough that the bond quality is not affected.

In order to relate the modal analysis results to the vibration displacement distribution measurement (Fig. 5), the details of the concentrator vibration at the computed working frequency (62.2 kHz—2nd axial mode) is investigated. Fig. 8 shows the computed relative displacement contour plots along the concentrator for the $+z$ (top view), $-z$ (bottom view), $-y$ (LHS view), and $+y$ (RHS view) components, respectively.

The computed displacement distribution patterns for the axial mode agree with the results measured by the interferometer, with the main nodes and antinodes being located at more or less similar locations (Fig. 10). This good agreement leads us to believe that, although other unwanted modes are also excited, they are small enough not to affect the main axial mode to a great extent and, hence, high quality bonding still can be maintained. Comparatively large errors are found in the top and bottom scannings, in which holes for threading the Al wires have been ignored in our FEM model, and the boundary condition for clamping the transducer has been simplified from a 3-line clamping to a fixed boundary. The geometrical simplification leads to errors near the holes because discontinuity of wave occurs at these locations.

Similar FEM simulation has been performed by other authors [14], and they also reported that, in addition to the axial mode, undesirable higher order flexural modes (the 13th flexural modes) exist near the transducer operating frequency and are excited simultaneously in a practical transducer system.

VI. Conclusions

The resonance characteristics of an ultrasonic transducer system used in our wire bonding system was found to be quite complicated when measured by an impedance analyzer. A heterodyne interferometer was used to measure the transducer vibration displacement distributions, and standing wave patterns were found along the surface of the concentrator. A FE model of this transducer was set up, and the frequencies of the first 120 allowable modes were computed. The displacement distributions of the 2nd axial mode agreed well with the value measured by interferometric method. Hence, the axial mode should be the dominant mode of the transducer. Undesirable non-axial modes, especially higher order flexural modes, also were found to occur in the transducer operating frequency range and are difficult to completely eliminate. The measured displacement distributions, therefore, are the resultant displacement of all the allowable modes being excited in the transducer. However, the excitations of these deleterious modes were found to be small enough, and good bonds can still be formed.

The results obtained in this work have been used in finding an appropriate location for piezoelectric sensors installation that satisfy the following criteria: sensor installed at this location will produce strong output, the sensor output should be sensitive to the change of boundary conditions at the tip of the wedge, and the location should be chosen such that the sensor would not be damaged during the bonding process. Based on these criteria, a piezoelectric sensor has been installed at 36 mm on the top part of the concentrator (Fig. 5) to monitor the bond quality during

Fig. 8. The computed relative displacement contour plots along the concentrator at the working frequency (62.2 kHz—2nd axial mode) for the (a) $+z$ (top view), (b) $-z$ (bottom view), (c) $-y$ (LHS view), and (d) $+y$ (RHS view) components, respectively.
Fig. 9. Relative displacement distributions of different vibration modes including: mode 59 (red line), mode 60 (yellow line), mode 61 (blue line), and mode 62 (green line). (a) Top scanning, (b) bottom scanning, (c) LHS scanning, and (d) RHS scanning. Note that amplitude of each mode is only relative, direct comparison should not be made with other modes as there is no absolute calibration,

TABLE I
THE COMPUTED MODES WITH FREQUENCIES WITHIN 5% OF THE MEASURED TRANSDUCER OPERATING FREQUENCY.

Computed mode number	Computed mode frequency (kHz)	Computed mode type
59	62.2	2nd axial mode
60	63.3	16th flexural (lateral) mode
61	63.8	12th flexural (vertical) mode
62	64.4	Complex flexural (lateral) and torsional mode

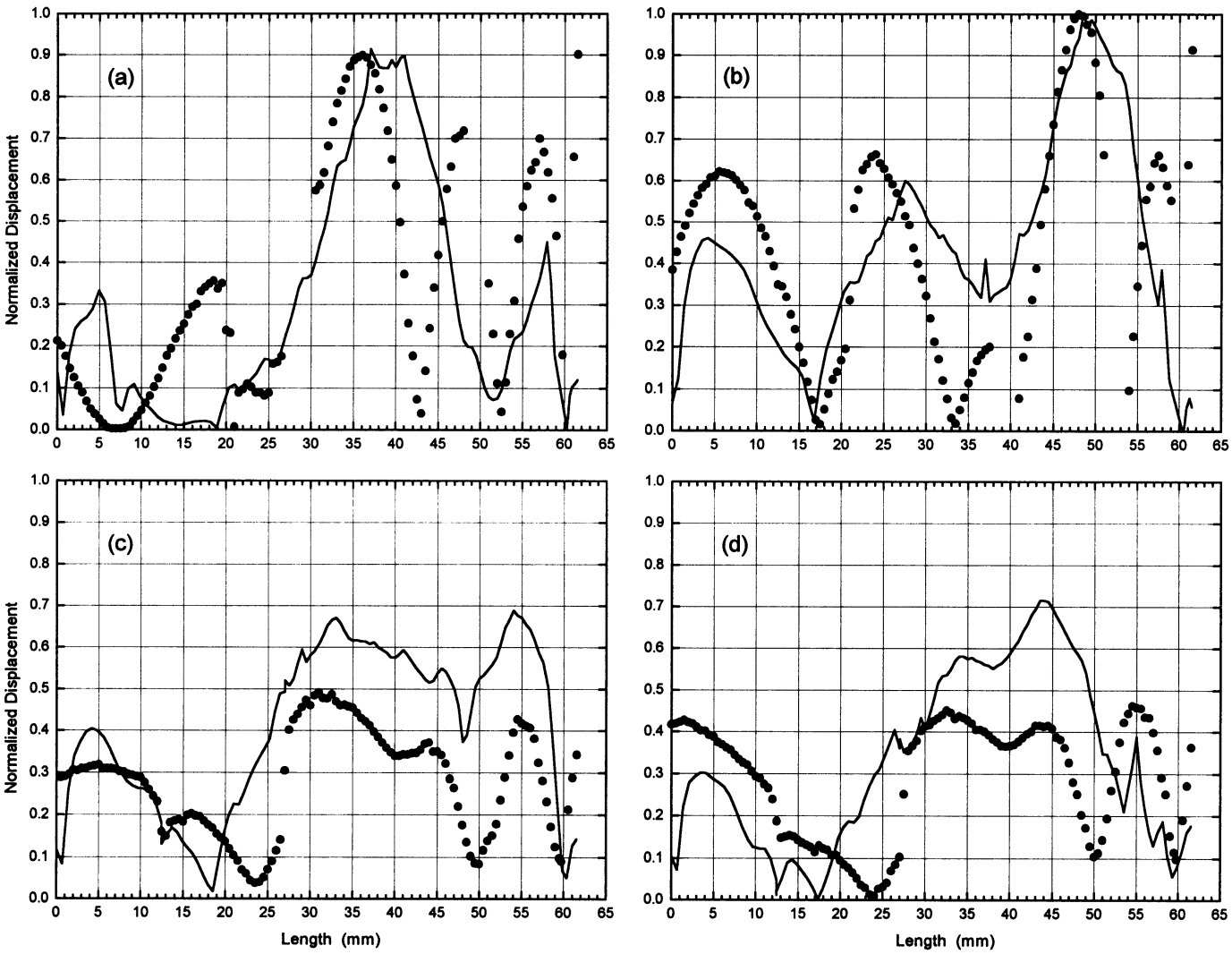

Fig. 10. Measured (solid circle) and computed (axial mode) (solid line) displacement distributions (normalized). (a) Top scanning, (b) bottom scanning, (c) LHS scanning, and (d) RHS scanning.

bonding. The sensor output signals are found to be very sensitive to the bond quality, and details of the monitoring system are reported in a separate paper [15].

Acknowledgments

The authors would like to thank the CAE group of ASM Assembly Automation Ltd., for their help in the finite element method analysis work.

References

[1] H. K. Charles, Jr., "Electrical interconnection," *Electronic Materials Handbook, vol. 1—Packaging*. ASM International, 1989, pp. 224–236.
[2] R. Rodwell and D. A. Worrall, "Quality control in ultrasonic wire bonding," *Hybrid Circuits*, no. 7, pp. 67–72, 1985.
[3] M. McBrearty, L. H. Kim, and N. M. Bilgutay, "Analysis of impedance loading in ultrasonic transducer systems," *Proc. IEEE Ultrason. Symp.*, 1988, pp. 497-502.
[4] N. M. Bilgutay, X. Li, and M. McBrearty, "Development of nondestructive bond monitoring techniques for ultrasonic bonders," *Ultrasonics*, vol. 24, pp. 307–317, Nov. 1986.
[5] L. G. Markulov and A. V. Kharitonov, "Theory and analysis of sectional concentrators," *Sov. Phys.—Acoust.*, vol. 5, pp. 183–190, 1959.
[6] E. A. Neppiras, "The pre-stressed piezoelectric sandwich transducer," in *Proc. Ultrason. Int. Conf.*, 1973, pp. 295–302.
[7] Z. Yan and Z. Lin, "Optimum design for sandwich transducer—by analyzing effects of structure and material parameters of transducer on its performance," *Acta Acust.*, vol. 20, no. 1, pp. 18–25, Jan. 1995.
[8] F. Graff, *Wave Motion in Elastic Solids*. Oxford, UK: Clarendon Press, 1975.
[9] S. W. Or, H. L. W. Chan, V. C. Lo, and C. W. Yuen, "Sensors for automatic process control of wire bonding," In: *Proc. 10th IEEE Int. Symp. Applications of Ferroelectrics (ISAF)*, 1996, vol. 2, pp. 991–994.
[10] D. Royer and E. Dieulesaint, "Optical probing of the mechanical impulse response of a transducer," *Appl. Phys. Lett.*, no. 49, pp. 1056–1058, 1986.
[11] B. Carlson, *Communication Systems—An Introduction to Signal and Noise in Electrical Communication*, 3rd ed. New York: McGraw-Hill, 1986, pp. 236–243.
[12] D. Royer and V. Kmetik, "Measurement of piezoelectric constants using an optical heterodyne interferometer," *Electron. Lett.*, vol. 28, pp. 1828–1830, 1992.
[13] R. D. Cook, *Finite Element Modeling for Stress Analysis*. New York: Wiley, 1995.
[14] R. B. Morris, P. Carnevali, and W. T. Bandy, "Dynamics of an ultrasonic bonding tool: A case study in P-version finite-element analysis," *J. Acoust. Soc. Amer.*, vol. 90, no. 6, pp. 2919–2923, 1991.
[15] S. W. Or, H. L. W. Chan, V. C. Lo, and C. W. Yuen, "Ultrasonic wire bond quality monitoring using piezoelectric sensor," *Sens. Actuators A: Physical*, vol. 65, pp. 69–75, 1998.

S. W. Or (M'97) was born in 1971. He received the Higher Diploma in Marine Communication and Electronic Technology, the B.Sc.(HONS.), and M.Phil. degrees in engineering physics from the Hong Kong Polytechnic University in 1992, 1995, and 1997, respectively. He is currently a research engineer at ASM Assembly Automation Ltd. in Hong Kong.

Mr. Or is a graduate member of the Institute of Physics, U.K.

H. L. W. Chan was born in 1948. She received the B.Sc. and M.Phil. degrees in physics from the Chinese University of Hong Kong in 1970 and 1974, respectively, and the Ph.D. degree in applied physics from Macquarie University, Australia, in 1987.

From 1987 to 1991, she worked as a research scientist at CSIRO Division of Applied Physics in Sydney and was responsible for setting up the standards for medical ultrasound in Australia. She then worked at GEC-Marconi Pty., Australia, for a year as a senior acoustic designer before returning to Hong Kong in 1992.

Dr. Chan is currently a professor in the Department of Applied Physics at the Hong Kong Polytechnic University.

V. C. Lo (M'96) was born in 1956. He received the B.Sc.(HONS.) and M.Phil. degrees in physics and the Ph.D. degree in electronic engineering from the Chinese University of Hong Kong in 1979, 1982, and 1991, respectively.

In 1982, he became an assistant lecturer in the Department of Applied Science at the Hong Kong Polytechnic University and was promoted to a lecturer in the Department of Applied Physics in 1984. Since 1992 he has been an assistant professor. His research interests include experimental investigation and theoretical modeling of semiconductor materials and devices.

Dr. Lo is a member of the Hong Kong Physical Society, the American Physical Society, USA, and the Materials Research Society, USA.

C. W. Yuen was born in 1965. He received the B.Sc.(HONS.) degree in electronic engineering from the City University of Hong Kong in 1989.

Mr. Yuen joined ASM Assembly Automation Ltd., Hong Kong in 1989. He is currently a principal engineer at ASM and is responsible for the development of electronic circuits and systems for industrial automation applications.